

Effect of the introduction of H atoms on magnetic properties and magnetic entropy change in metamagnetic Heusler alloys Ni–Mn–In

F. X. Hu,^{a)} J. Wang, L. Chen, J. L. Zhao, J. R. Sun, and B. G. Shen

State Key Laboratory of Magnetism, Institute of Physics, Chinese Academy of Sciences, Beijing 100190, People's Republic of China

(Received 20 June 2009; accepted 25 August 2009; published online 16 September 2009)

By hydrogen insertion into $\text{Ni}_{51}\text{Mn}_{49-x}\text{In}_x$ ($x=16.2, 16.6$) Heusler alloys, the interstitial compounds $\text{Ni}_{51}\text{Mn}_{49-x}\text{In}_x\text{H}_\delta$ were fabricated. The introduction of H atoms does not change the $L2_1$ structure of the alloys but shifts martensitic temperature (T_M) to lower temperature. Magnetic measurements indicated the hydrogenated $\text{Ni}_{51}\text{Mn}_{49-x}\text{In}_x\text{H}_\delta$ compounds retain the metamagnetic properties although the ferromagnetic behavior of martensitic phases is slightly enhanced due to the introduction of H atoms. The strong metamagnetic behaviors result in large magnetocaloric effect (MCE). By controlling H content an extended temperature range having large MCE can be achieved. © 2009 American Institute of Physics. [doi:10.1063/1.3229890]

More and more interests have been focused on the magnetic refrigerant investigations since the recent discovery of several giant magnetocaloric materials, such as GdSiGe ,¹ MnFePAs ,² LaFeSi ,^{3,4} and NiMnGa ,^{5,6} etc. Among these materials, the hydrogenated $\text{La}(\text{Fe}, \text{Si})_{13}\text{H}_\alpha$ compounds have attracted much attention.^{4,7} The introduction of interstitial H atoms enhances the ferromagnetic exchange interaction. The Curie temperature T_C can be easily pushed to room temperature while keeping the large magnitude of magnetocaloric effect (MCE).

Ferromagnetic Heusler alloys with $L2_1$ structure have been well-known for quite a long time because of their ferromagnetic shape memory effect (FSME). For the conventional Heusler alloys, FSME is realized through the field-induced rearrangement of martensite variants. The driving force comes from magnetocrystalline anisotropy energy (MAE), which is orientation dependent and limited with a saturation magnetic field.⁸ A recent discovery of metamagnetic shape memory alloys⁹ has stirred intense interests because of the huge shape memory effect and its different mechanism from the traditional ferromagnetic Heusler alloys. An abrupt change of magnetization across martensitic transition results in a large Zeeman energy $\mu_0\Delta M \cdot H$, which drives the structural transformation and causes a field-induced metamagnetic behavior. Unlike MAE, Zeeman energy does not strongly depend on crystal orientation and increases continuously with the field, thus the resulted metamagnetic shape memory effect (MSME) can be huge.⁸ The simultaneous changes of magnetism and structure induced by magnetic field satisfy the demands posed on the magnetic properties of active magnetocaloric materials. Naturally, attentions were attracted soon on the MCE in such MSME alloys^{6,10} In these materials, any subtle changes of Mn–Mn atomic distance and chemical surroundings of Mn atoms will influence the magnetic properties, and thus affect MCE. Inserting interstitial atoms is expected to influence their properties through disturbing the Mn–Mn atomic distance and the surroundings, which may provide a useful way to tune the magnetic properties and martensitic transition temperature, and thus the magnetocaloric effect. However,

up to now rare investigations on interstitial Heusler alloys have been reported. In this letter, we report the effect of the introduction of H atoms on magnetic properties and magnetic entropy change in metamagnetic Heusler alloys $\text{Ni}_{51}\text{Mn}_{49-x}\text{In}_x$.

$\text{Ni}_{51}\text{Mn}_{49-x}\text{In}_x$ ($x=16.2, 16.6$) samples were prepared by arc-melting technique.¹¹ The hydrogen absorption was performed by annealing the samples under hydrogen gas atmosphere in commercial P-C-T (pressure-composition-temperature) apparatus. By adjusting gas pressure and annealing temperature the hydrogen concentration δ in $\text{Ni}_{51}\text{Mn}_{49-x}\text{In}_x\text{H}_\delta$ can be controlled and determined in the P-C-T apparatus. X-ray diffraction (XRD) experiments were carried out to identify the structure. It was found that the hydrogenated samples still remain in the $L2_1$ structure but the lattice parameter is enlarged. Inset of Fig. 1 displays XRD patterns of $\text{Ni}_{51}\text{Mn}_{32.4}\text{In}_{16.6}\text{H}_{5.2}$ and $\text{Ni}_{51}\text{Mn}_{32.4}\text{In}_{16.6}$ collected at room temperature. Both of them exhibit cubic $L2_1$ structure. The lattice parameter of former (0.600 31 nm) is slightly larger than that of latter (0.599 70 nm). A slight splitting of (220) peak is observed for the both samples, which may be related to the early stage of the martensitic phase.¹² All magnetic measurements were performed using a superconducting quantum interference device (SQUID) magnetometer.

Shown in Fig. 1 are the zero-field-cooled (ZFC) and field-cooled (FC) magnetizations¹³ as functions of temperature (M - T) under different fields of 0.05 T, and 5 T for $\text{Ni}_{51}\text{Mn}_{32.4}\text{In}_{16.6}$ and $\text{Ni}_{51}\text{Mn}_{32.4}\text{In}_{16.6}\text{H}_{5.2}$ samples. The magnetization anomaly at ~ 303 K in M - T curve under 0.05 T for $\text{Ni}_{51}\text{Mn}_{32.4}\text{In}_{16.6}$ corresponds to the ferromagnetic ordering temperature T_C of austenitic phase (denoted as T_C^A thereafter). A nearly same T_C^A is also found in $\text{Ni}_{51}\text{Mn}_{32.4}\text{In}_{16.6}\text{H}_{5.2}$ hydride, indicating that the introduction of H atoms does not strongly influence the ferromagnetic interaction of austenitic phase. With decreasing temperature, an abrupt decrease of magnetization occurs at ~ 249 K for $\text{Ni}_{51}\text{Mn}_{32.4}\text{In}_{16.6}$, corresponding to the martensitic transition temperature T_M . (Here, both T_M and T_C^A are defined as the temperature corresponding to the maximal slope of M - T curve under 0.05 T on cooling.) Similar to the observations in the close compositions $\text{Ni}_{51}\text{Mn}_{49-x}\text{In}_x$ (x

^{a)}Electronic mail: hufx@g203.iphy.ac.cn.

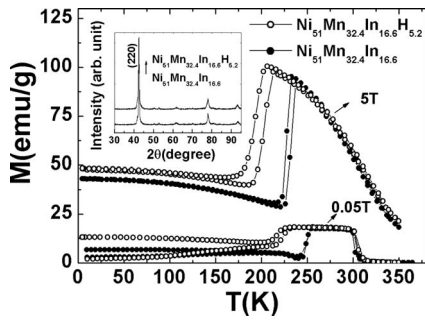


FIG. 1. Temperature dependent ZFC and FC magnetization measured under different fields of 0.05 and 5 T for $\text{Ni}_{51}\text{Mn}_{32.4}\text{In}_{16.6}$ and $\text{Ni}_{51}\text{Mn}_{32.4}\text{In}_{16.6}\text{H}_{5.2}$ samples. The inset shows XRD patterns collected at room temperature for the two samples.

$= 15.6, 16.0, 16.2$),¹¹ the thermal hysteresis around T_M for $\text{Ni}_{51}\text{Mn}_{32.4}\text{In}_{16.6}$ is small, < 2 K, and less than 4 K even under a magnetic field of 5 T. For the hydrogenated $\text{Ni}_{51}\text{Mn}_{32.4}\text{In}_{16.6}\text{H}_{5.2}$, the temperature hysteresis is slightly strengthened upon hydrogen absorption: about 5 K under 0.05 T, and ~ 10 K when a 5 T magnetic field is applied. At low temperatures, a large separation between ZFC and FC magnetization under 0.05 T is observed for the two samples, which can be understandable taking into account the magnetic anisotropy and antiferromagnetic exchange between Mn–Mn nearest neighbors in the martensitic state.^{14,15}

A fascinating phenomenon is that the insertion of H atoms shifts T_M to lower temperature. For the hydrogenated $\text{Ni}_{51}\text{Mn}_{32.4}\text{In}_{16.6}\text{H}_{5.2}$, the T_M appears at ~ 217 K, lower than that of $\text{Ni}_{51}\text{Mn}_{32.4}\text{In}_{16.6}$ by ~ 32 K. Another feature is that the saturated magnetization of martensitic phases is enhanced due to the introduction of H atoms while that of austenitic phases remains nearly unchanged. The magnetization of $\text{Ni}_{51}\text{Mn}_{32.4}\text{In}_{16.6}\text{H}_{5.2}$ at 5 K is ~ 48.4 emu/g under 5 T, larger than that of $\text{Ni}_{51}\text{Mn}_{32.4}\text{In}_{16.6}$ (~ 43.2 emu/g) by 12%. One can also find that, from Fig. 1, the T_M for the both samples behaves high sensitivity to external field. A 5 T magnetic field shifts T_M from 249 to 228 K at a rate of 4.2 K/T for $\text{Ni}_{51}\text{Mn}_{32.4}\text{In}_{16.6}$, and from 217 to 193 K at a rate of 4.8 K/T for $\text{Ni}_{51}\text{Mn}_{32.4}\text{In}_{16.6}\text{H}_{5.2}$. Although the magnetization difference across martensitic transition, ΔM , is somewhat reduced by inserting the interstitial H atoms, the driving rate of T_M by a magnetic field shows a small increase. It indicates that the insertion of H atoms make the martensitic transition easier to be driven under the same Zeeman energy. The different effect of inserting H atoms on the magnetization of martensitic and austenitic phases is worthy to pay more attention and will be discussed below.

The magnetic interaction is quite complex in the off-stoichiometric alloys Ni–Mn–Z especially for the ones with an excess of Mn.¹⁶ In these cases, a smaller Mn–Mn distance of around ~ 0.29 nm appears, leading to an antiferromagnetic coupling. Recent neutron-polarization-analysis experiments confirmed¹⁷ that the magnetic correlations are antiferromagnetic at temperatures lower than T_M for $\text{Ni}_{50}\text{Mn}_{40}\text{Sb}_{10}$ and $\text{Ni}_{50}\text{Mn}_{37}\text{Sn}_{13}$. We also noted that the true magnetic ordering can be various, depending on the actual compositions. In samples $\text{Ni}_{50}\text{Mn}_{35}\text{Sn}_{15}$, $\text{Ni}_{50}\text{Mn}_{37}\text{Sb}_{13}$, the shortest Mn–Mn distance is 0.2998 and 0.2989 nm, respectively. Both of them display antiferromagnetic properties. However, $\text{Ni}_{50}\text{Mn}_{34}\text{In}_{16}$ has a shortest Mn–Mn distance of 0.3004 nm, showing ferromagnetism.¹⁸ It is evident that a very small

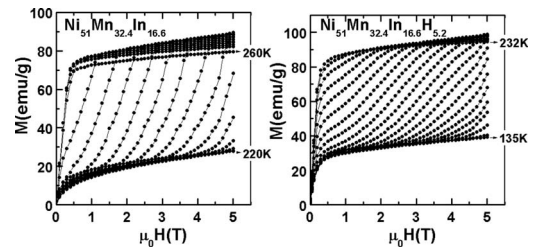


FIG. 2. The magnetization isotherms M - H collected on field increase for $\text{Ni}_{51}\text{Mn}_{32.4}\text{In}_{16.6}$ and $\text{Ni}_{51}\text{Mn}_{32.4}\text{In}_{16.6}\text{H}_{5.2}$ samples. The temperature step around T_M is 2 K.

change of the Mn–Mn distance will greatly affect the magnetic properties of the sample. In present $\text{Ni}_{51}\text{Mn}_{32.4}\text{In}_{16.6}$, the authentic phase shows strong ferromagnetic properties, indicating that Mn–Mn ferromagnetic exchange dominates the authentic state. In this case, a small change of Mn–Mn distance caused by the insertion of H atoms may not significantly influence the ferromagnetic properties. As observed in our experiments, the T_C^A and saturated magnetization remain nearly unchanged upon H doping. However, for the martensitic state of present $\text{Ni}_{51}\text{Mn}_{32.4}\text{In}_{16.6}$, because of the different crystalline symmetry from the authentic state, the Mn–Mn antiferromagnetic coupling will play a key role in determining the magnetic properties. The introduction of H atoms elongates Mn–Mn distance, making the system favor the ferromagnetic coupling and thus leading to an enhancement of saturated magnetization of martensitic state.

On the other hand, valence electron concentration, e/a , is a critical factor that influences martensitic transformation behavior and magnetic properties. In NiMn-based Heusler alloys, T_M behaves strongly dependent on e/a and rapidly decreases with decreasing e/a .¹³ The addition of H may also affect the T_M by altering e/a . Scarce reports appear on the hybridization between the $1s$ electron of interstitial H atom and the d -bands of Ni, Mn metals. Fortunately, Itsumi *et al.*¹⁹ carried out electronic structure calculations for bcc Fe with interstitial H by using the first principles discrete variational method. This work indicated that volume expansion is expected because the interstitial H feels a repulsive force, and Fe–H interaction occurs mainly via the Fe $4s$ and H $1s$ orbitals. Charge transfer of $\sim 0.6e$ from Fe onto H leads to a decrease in metallic bond strength. With the assumption of the similarity to the case in Fe–H systems, the addition of H into NiMnIn might also make the system less metallic and thus cause a decrease in e/a . In accordance with the general dependence of T_M on e/a , T_M decreases with H doping.

Shown in Fig. 2 are the magnetization isotherms M - H on field increase for $\text{Ni}_{51}\text{Mn}_{32.4}\text{In}_{16.6}$ and $\text{Ni}_{51}\text{Mn}_{32.4}\text{In}_{16.6}\text{H}_{5.2}$. The temperature step around T_M is 2 K. Above a critical field H_C , a sharp change of magnetization occurs for the both samples, which indicates that a field-induced metamagnetic transition from a martensitic to an austenitic state takes place. The critical field H_C increases with decreasing temperature, which predicts that the ΔS peak will broaden to lower temperature. Based on the magnetization data in Fig. 2, magnetic entropy change ΔS was calculated by using Maxwell relation.^{1–6,20} Fig. 3 displays ΔS as functions of temperature and magnetic field for both samples. One can note that ΔS of both samples is positive. With increasing magnetic field, ΔS peak gradually broadens toward lower temperatures. The maximum of ΔS reaches 17.2 and 13.0

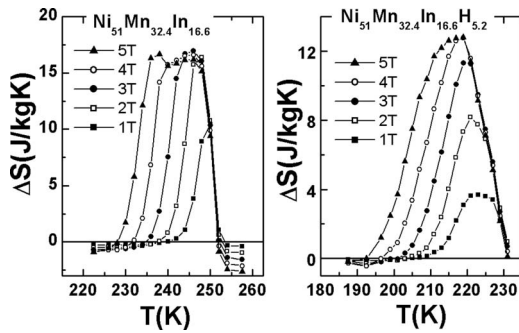


FIG. 3. Magnetic entropy change ΔS as a function of temperature under different magnetic fields for $\text{Ni}_{51}\text{Mn}_{32.4}\text{In}_{16.6}$ and $\text{Ni}_{51}\text{Mn}_{32.4}\text{In}_{16.6}\text{H}_{5.2}$ samples.

J/kg K at 246 and 219 K, and the temperature span of ΔS attains to 17 and 22.5 K under a 5 T field for $\text{Ni}_{51}\text{Mn}_{32.4}\text{In}_{16.6}$ and $\text{Ni}_{51}\text{Mn}_{32.4}\text{In}_{16.6}\text{H}_{5.2}$, respectively. For the hydrogenated sample, the ΔS magnitude becomes somewhat smaller but the temperature span becomes wider. The refrigerant capacity, $\text{RC} = \int_{T_1}^{T_2} \Delta S(T)_H dT$, evaluated from the integration over the full width at half maximum in a ΔS - T curve, remains nearly unchanged compared to the one without H (~ 250 J/kg). The ΔS shows a tablelike peak under 5 T for both samples. It should reflect the intrinsic nature of magneto-caloric effect.^{11,21}

Our studies also indicated that the H content can be controlled by adjusting annealing temperature and gas pressure. For a close composition $\text{Ni}_{51}\text{Mn}_{32.8}\text{In}_{16.2}$, the H content was controllably tuned to be $\delta=1.4$. Figure 4 displays the ZFC-FC magnetization under different fields of 0.05 T, and 5 T and magnetic entropy change ΔS as functions of temperature and magnetic field for both $\text{Ni}_{51}\text{Mn}_{32.8}\text{In}_{16.2}$ and $\text{Ni}_{51}\text{Mn}_{32.8}\text{In}_{16.2}\text{H}_{1.4}$. One can find that similar shift of T_M to lower temperature and enhancement of the saturated magnetization of martensitic phase occur in $\text{Ni}_{51}\text{Mn}_{32.8}\text{In}_{16.2}\text{H}_{1.4}$ hydride. However, due to the small amount of H atoms, the shift of T_M is just around 6 K. This result suggests that one could tune the T_M (and thus the peak of ΔS) by controlling the content of interstitial H atoms. The maximum of ΔS is

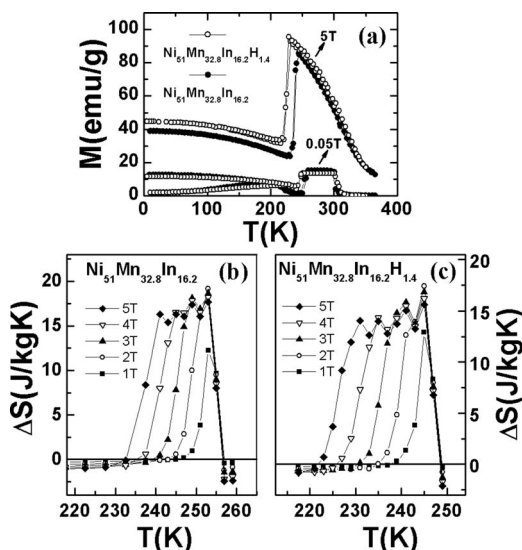


FIG. 4. (a) Temperature dependent ZFC and FC magnetization measured under different fields of 0.05 T and 5 T, and magnetic entropy change ΔS as a function of temperature under different magnetic fields for (b) $\text{Ni}_{51}\text{Mn}_{32.8}\text{In}_{16.2}$ and (c) $\text{Ni}_{51}\text{Mn}_{32.8}\text{In}_{16.2}\text{H}_{1.4}$ samples.

19.2 and 17.5 J/kg K at 253 and 245 K, and the temperature span of ΔS attains to 17 and 20 K under a 5 T field for $\text{Ni}_{51}\text{Mn}_{32.8}\text{In}_{16.2}$ and $\text{Ni}_{51}\text{Mn}_{32.8}\text{In}_{16.2}\text{H}_{1.4}$, respectively. Similar to the case in $\text{Ni}_{51}\text{Mn}_{32.4}\text{In}_{16.6}$, upon H doping the ΔS magnitude is slightly reduced while the temperature span becomes wider. The evaluated refrigerant capacity RC remains nearly unchanged upon H doping.

In summary, interstitial H atoms were introduced in the metamagnetic shape memory alloys $\text{Ni}_{51}\text{Mn}_{49-x}\text{In}_x$ ($x = 16.2, 16.6$). The introduction of H atoms shifts martensitic temperature T_M to lower temperature and enhances the saturated magnetization of martensitic phase. Through adjusting H content, T_M , at which ΔS peaks, can be controlled. Upon H doping the ΔS magnitude is slightly reduced, but the temperature span is broadened and thus the refrigerant capacity RC remains nearly unchanged. All these suggest that the hydrogenated $\text{Ni}_{51}\text{Mn}_{49-x}\text{In}_x\text{H}_\delta$ can be promising candidates as magnetic refrigerants working in a wide temperature range. NiMn-based Heusler alloys are well-known for their multifunctional properties. The introduction of interstitial atoms may open an avenue for exploiting versatile applications.

This work has been supported by the National Natural Science Foundation of China, Hi-Tech Research and Development program of China, the Knowledge Innovation Project of the Chinese Academy of Sciences, and the National Basic Research of China.

- ¹V. K. Pecharsky and K. A. Gschneidner, Jr., *Phys. Rev. Lett.* **78**, 4494 (1997).
- ²O. Tegus, E. Brück, K. H. J. Buschow, and F. R. de Boer, *Nature (London)* **415**, 150 (2002).
- ³F. X. Hu, B. G. Shen, J. R. Sun, Z. H. Cheng, G. H. Rao, and X. X. Zhang, *Appl. Phys. Lett.* **78**, 3675 (2001).
- ⁴A. Fujita, S. Fujieda, Y. Hasegawa, and K. Fukamichi, *Phys. Rev. B* **67**, 104416 (2003).
- ⁵F. X. Hu, B. G. Shen, and J. R. Sun, *Appl. Phys. Lett.* **76**, 3460 (2000).
- ⁶T. Krenke, E. Duman, M. Acet, E. F. Wassermann, X. Moya, L. Mañosa, and A. Planes, *Nature Mater.* **4**, 450 (2005).
- ⁷Y. F. Chen, F. Wang, B. G. Shen, F. X. Hu, J. R. Sun, G. J. Wang, and Z. H. Cheng, *J. Phys. Condens. Matter* **15**, L161 (2003).
- ⁸H. E. Karaca, I. Karaman, B. Basaran, Y. Ren, Y. I. Chumlyakov, and H. J. Maier, *Adv. Funct. Mater.* **19**, 983 (2009).
- ⁹R. Kainuma, Y. Imano, W. Ito, Y. Sutou, H. Morito, S. Okamoto, O. Kitakami, K. Oikawa, A. Fujita, T. Kanomata, and K. Ishida, *Nature (London)* **439**, 957 (2006).
- ¹⁰Z. D. Han, D. H. Wang, C. L. Zhang, H. C. Xuan, B. X. Gu, and Y. W. Du, *Appl. Phys. Lett.* **90**, 042507 (2007).
- ¹¹F. X. Hu, J. Wang, J. Shen, B. Gao, J. R. Sun, and B. G. Shen, *J. Appl. Phys.* **105**, 07A940 (2009).
- ¹²M. Khan, I. Dubenko, S. Stadler, and N. Ali, *J. Appl. Phys.* **97**, 10M304 (2005).
- ¹³F. X. Hu, X. L. Qian, G. J. Wang, J. Wang, J. R. Sun, X. X. Zhang, Z. H. Cheng, and B. G. Shen, *J. Phys.: Condens. Matter* **15**, 3299 (2003).
- ¹⁴T. Krenke, M. Acet, E. Wassermann, X. Moya, L. Mañosa, and A. Planes, *Phys. Rev. B* **73**, 174413 (2006).
- ¹⁵S.-Y. Chu, A. Cramb, M. De Graef, D. Laughlin, and M. E. McHenry, *J. Appl. Phys.* **87**, 5777 (2000).
- ¹⁶Y. Sutou, Y. Imano, N. Koeda, T. Omori, R. Kainuma, K. Ishida, and K. Oikawa, *Appl. Phys. Lett.* **85**, 4358 (2004).
- ¹⁷S. Aksoy, M. Acet, P. P. Deen, L. Mañosa, and A. Planes, *Phys. Rev. B* **79**, 212401 (2009).
- ¹⁸S. Y. Yu, Z. X. Cao, L. Ma, G. D. Liu, J. L. Chen, G. H. Wu, B. Zhang, and X. X. Zhang, *Appl. Phys. Lett.* **91**, 102507 (2007).
- ¹⁹Y. Itsumi and D. E. Ellis, *J. Mater. Res.* **11**, 2206 (1996).
- ²⁰A. M. Tishin and Y. I. Spichkin, *The Magnetocaloric Effect and Its Applications* (Institute of Physics, Bristol, 2003).
- ²¹G. J. Liu, J. R. Sun, J. Shen, B. Gao, H. W. Zhang, F. X. Hu, and B. G. Shen, *Appl. Phys. Lett.* **90**, 032507 (2007).